NATIONAL ADVISORY COMMITTEE FOR AERONAUTICS

TECHNICAL MEMORANDUM 1373

ON FORCE-DEFLECTION DIAGRAMS OF AIRPLANE SHOCK ABSORBER STRUTS

FIRST, SECOND, AND THIRD PARTIAL REPORTS*

By K. Schlaefke

*Translation of "Zur Kenntnis der Kraftwegdiagramme von Flugzeugfederbeinen." Technische Berichte, Bd. 11, Hefts 2, 4, and 5, 1944.

NACA

Washington

November 1954

1T

NATIONAL ADVISORY COMMITTEE FOR AERONAUTICS

TECHNICAL MEMORANDUM 1373

ON FORCE-DEFLECTION DIAGRAMS OF AIRPLANE SHOCK ABSORBER STRUTS

FIRST PARTIAL REPORT - COMPARISON OF DIAGRAMS WITH LINEAR AND QUADRATIC DAMPING*

By K. Schlaefke

Summary: The investigations - in an earlier publication - concerning force-deflection diagrams of airplane shock-absorber struts with linear damping are repeated with the assumption that the damping be proportional to the square of the spring-compression velocity. The diagrams with quadratic damping essentially differ from those with linear damping. The comparison with drop-hammer diagrams that had been plotted shows that the damping actually depends linearly, or at least almost linearly, on the spring-compression velocity.

The unsolved problems in undercarriage construction are still so numerous that, like a hydra, from each problem that has been solved, two new ones grow out. Thus my present investigation is an outgrowth of a previous report (ref. 1) on the comparison of "buffered" shocks with "unbuffered shocks"; however, it encompasses only a single additional problem. On the other questions that arose I hope to report in sequence later on.[1]

The present investigation thus repeats the considerations reported in said treatise with the difference that here a damping is assumed which is proportional to the square of the spring compression velocity, while there we dealt with linear damping. While I have found no direct reference in the literature as regards to the type of damping expectable in airplane spring struts, personal experiences and oral communications from outside sources would indicate that the linear damping was set up mainly with respect to mathematical treatment and only as a second thought with respect to physical correctness. Thus the calculatory treatment of double-springings, such as spring struts with quadratic damping and tires, offers insurmountable difficulties, whereas with linear damping an exact mathematical treatment is possible (ref. 2).

---

*"Zur Kenntnis der Kraftwegdiagramme von Flugzeugfederbeinen, 1. Teilbericht: Vergleich von Diagrammen mit linearer und quadratischer Dämpfung." Technische Berichte, Bd. 11, Heft 2, Feb. 15, 1944, pp. 51-53.

[1]NACA editor's note: Subsequent papers in this series are included in this translation as Second and Third Partial Reports.

In the following, therefore, the force-deflection diagram with quadratic damping shall be compared with linear damping in order to gain a perspective of the physical relationships therein.

The energy equation for the first spring shock (using the same assumptions and designations of the previous report) is

$$\int P\,df = \int \left(P_v + cf + k_2 v^2\right) df$$
$$= \frac{M}{2}\left(v_0^2 - v^2\right) + (Mg - L)f \tag{1}$$

From equation (1) with

$$\left.\begin{aligned} \frac{c}{M} &= \omega^2, \qquad \frac{k_2}{M} = \frac{2\omega^2\vartheta_2}{g}, \\ \frac{Mg - L - P_v}{Mg} &= 1 - \lambda - \sigma = \alpha, \\ v &= \varphi\,\frac{g}{\omega}, \qquad f = \psi\,\frac{g}{\omega^2} \end{aligned}\right\} \tag{2}$$

one obtains, after differentiation with respect to f

$$\frac{d\left(v^2\right)}{df} + \frac{4\omega^2\vartheta_2}{g}\,v^2 + 2\omega^2 f - 2g\alpha = 0 \tag{3a}$$

or

$$\frac{d\left(\varphi^2\right)}{d\psi} + 4\vartheta_2\varphi^2 + 2(\psi - \alpha) = 0 \tag{3b}$$

The general solution (ref. 3) of the differential equation (3b) reads

$$\varphi^2 = Ae^{-\delta\psi} + B\psi + C \tag{4}$$

When inserting the solution (4) into the initial equation (3b) we obtain

$$Ae^{-\delta\psi}\left(-\delta + 4\vartheta_2\right) + \psi\left(4\vartheta_2 B + 2\right) + \left(B + 4\vartheta_2 C - 2\alpha\right) = 0 \tag{5}$$

The parentheses must disappear if equation (5) should be fulfilled for every value of ψ. Thus is obtained

$$\left.\begin{aligned} \delta &= 4\vartheta_2 \\ B &= -\frac{1}{2\vartheta_2} \\ C &= \frac{1}{2\vartheta_2}\left(\alpha + \frac{1}{4\vartheta_2}\right) \end{aligned}\right\} \tag{6}$$

The constant A is derived from the initial condition

$$\varphi^2_{(\psi=0)} = \varphi_0{}^2 \tag{7}$$

as

$$A = \varphi_0{}^2 - \frac{1}{2\vartheta_2}\left(\alpha + \frac{1}{4\vartheta_2}\right) \tag{8}$$

With equations (6) and (8), the solution (4) is written in final form

$$\varphi^2 = \left(\varphi_0{}^2 - \frac{1}{2\vartheta_2}\left(\alpha + \frac{1}{4\vartheta_2}\right)\right)e^{-4\vartheta_2\psi} - \frac{1}{2\vartheta_2}\psi + \frac{1}{2\vartheta_2}\left(\alpha + \frac{1}{4\vartheta_2}\right) \tag{9}$$

When setting approximately

$$e^{-4\vartheta_2\psi} \approx 1 \tag{10}$$

which is permissible for low dampings, we obtain

$$\varphi^2 \approx \varphi_0{}^2 - \frac{1}{2\vartheta_2}\psi \tag{11}$$

and with

$$0 \approx \varphi_0{}^2 - \frac{1}{2\vartheta_2}\psi_g \tag{12}$$

finally

$$\varphi^2 \approx \varphi_0{}^2\left(1 - \frac{\psi}{\psi_g}\right) \tag{13}$$

Thus, for not too great dampings, the square of the spring compression velocity decreases linearly with the spring stroke.

In order to determine the maximum deflection ψ_g, $\varphi^2 = 0$ is inserted into equation (9), and thus obtain

$$\psi_g - \left(\alpha + \frac{1}{2\vartheta_2}\right) - \left(2\vartheta_2\varphi_0{}^2 - \left(\alpha + \frac{1}{4\vartheta_2}\right)\right)e^{-4\vartheta_2\psi_g} = 0 \tag{14}$$

an equation which may be solved by trial only.

The maximum spring stroke may be determined with another method of approach as well.

$$J = \int_0^{\psi_g} S\, d\psi = \frac{\varphi_0{}^2}{2} + \psi_g(1 - \lambda) \tag{15}$$

When calculating the integral, we obtain

$$J = \int_0^{\psi_g} \left(\sigma + \psi + 2\vartheta_2\varphi^2\right)d\psi = \psi_g\left(\sigma + \alpha + \frac{1}{4\vartheta_2}\right) + \frac{2\vartheta_2\varphi_0{}^2 - \left(\alpha + \frac{1}{4\vartheta_1}\right)}{4\vartheta_2}\left(1 - e^{-4\vartheta_2\psi_g}\right) \tag{16}$$

According to equation (2)

$$\sigma + \alpha = 1 - \lambda \tag{17}$$

and therewith one obtains, equating equations (15) and (16), likewise equation (14).

As already established in equation (16), the force S is

$$S = \frac{P}{Mg} = \frac{P_v + cf + k_2 v^2}{Mg} = \sigma + \psi + 2\vartheta_2 \varphi^2 \tag{18}$$

The maximum value S_g is obtained by a zero-setting of the differential quotient. We then have

$$\frac{dS}{d\psi} = 1 + 2\vartheta_2 \left(\frac{d(\varphi^2)}{d\psi} \right)_* = 0 \tag{19}$$

or

$$\left(\frac{d(\varphi^2)}{d\psi} \right)_* = - \frac{1}{2\vartheta_2} \tag{20}$$

When inserting equation (20) into equation (3b), we obtain

$$\varphi_*{}^2 = \frac{1}{2\vartheta_2} \left(\frac{1}{4\vartheta_2} - (\psi_* - \alpha) \right) \tag{21}$$

The insertion of equation (21) into equation (4) leads to

$$\frac{1}{2\vartheta_2} \left(\frac{1}{4\vartheta_2} - (\psi_* - \alpha) \right) = Ae^{-\delta\psi_*} + B\psi_* + C \tag{22}$$

or, according to equation (6), in general

$$B\psi + C = \frac{1}{2\vartheta_2} \left(\frac{1}{4\vartheta_2} - (\psi - \alpha) \right) \tag{23}$$

to the condition

$$Ae^{-\delta\psi_*} = 0 \tag{24}$$

This implies that S steadily increases further with ψ and finally reaches its optimum for $\psi = \infty$. For that reason the highest value of S is expectable in the force-deflection diagram at $\psi = \psi_g$, or $f = f_g$, respectively. Thus we have

$$S_g = \sigma + \psi_g \tag{25}$$

Finally, the springing effectiveness η is given by the equation

$$\eta = \frac{\frac{{\varphi_0}^2}{2\psi_g} + 1 - \lambda}{\sigma + \psi_g} \tag{26}$$

The component of the force S caused by damping is, according to equation (18)

$$D = 2\vartheta_2\varphi^2 = \left(D_0 - \left(\alpha + \frac{{\varphi_0}^2}{2D_0}\right)\right)e^{-\frac{2D_0}{{\varphi_0}^2}\psi} - \psi + \left(\alpha + \frac{{\varphi_0}^2}{2D_0}\right) \tag{27}$$

when the damping force at the start of the spring shock is expressed thus:

$$D_0 = 2\vartheta_2{\varphi_0}^2 \tag{28}$$

From equation (27), $\alpha = 0$, that is, $\lambda + \sigma = 1$, a variation of the damping force D is obtained as shown in figure 1. It is seen that, for finite values of the damping also, the course of D as function of ψ does not depart essentially from a straight line. With the assumption that

$$D_0 - \left(\alpha + \frac{{\varphi_0}^2}{2D_0}\right) = 0 \tag{29}$$

or

$$D_0 = D_{0crit} = \frac{\alpha}{2} + \sqrt{\frac{\varphi_0^2}{2} + \frac{\alpha^2}{4}} \tag{30}$$

D as a function of the spring stroke is exactly a straight line for which the equation reads

$$D = D_{0crit} - \psi \tag{31}$$

For $\alpha = 0$ this occurs for $D_{0crit} = \frac{\varphi_0}{2}\sqrt{2}$ as is shown by the line for $D_0 = 5$ and $\varphi_0^2 = 50$. When $D_0 < D_{0crit}$, the damping curve is concave toward the coordinate origin ($D_0 = 1$ and 2, $\varphi_0^2 = 10$ and 50). If $D_0 > D_{0crit}$, then the curve is bent toward the zero-point ($D_0 = 5$, $\varphi_0^2 = 10$).

From equations (14) and (28) we obtain, with $\varphi_0^2 = 50$ as well as with $\sigma = 0$ and $\lambda = 1$, that is, $\alpha = 0$, the variation of ψ_g as a function of the initial force D_0, as shown in figure 2. The latter serves as a foundation for plotting the force-deflection diagrams of figure 3.

Corresponding to the linear damping expectable with airplane spring struts, we obtain with $\varphi_0^2 = 50$ and $\vartheta_1 = 0.25$, from my previous report (ref. 1, eqs. (13a), (17a), and (20))

$$\left.\begin{aligned} \psi_{g1} &= 5.0313 \\ \psi_* &= 4.325 \\ S_{g1} &= 5.7325 \end{aligned}\right\} \tag{32}$$

The diagram d plotted for linear damping was made with the above values. As a comparison therewith were shown the three diagrams a, b, and c for quadratic damping.

Diagram a shows the same maximum force S_g as the diagram d, whereas diagram b begins with the same damping force D_0. Finally, diagram c has the same maximum spring stroke as diagram d. In figure 2, the points defining the relationship between ψ_g and D_0 are indexed with the letters of the diagram.

Thus, the form of the force-deflection diagrams with quadratic damping is essentially different from those of linear damping. The diagrams obtained in drop tests, however, have a similar appearance as diagram d, from which we may conclude that the actual damping of airplane spring struts is exactly, or at least very nearly, proportional to the spring compression velocity.

According to this understanding the quadratic damping thus has probably not too great a practical importance and it has been found sufficient to calculate further on with the compression spring velocity course as was given in equation (13).

For unchanged energy absorption then the approximation value ψ_{gn} is derived from the equation

$$\frac{2\sigma + \psi_{gn} + D_0}{2} \psi_{gn} = \frac{\varphi_0^2}{2} + \psi_{gn}(1 - \lambda) \tag{33}$$

as follows

$$\psi_{gn} = -\left(\frac{D_0}{2} - \alpha\right) + \sqrt{\varphi_0^2 + \left(\frac{D_0}{2} - \alpha\right)^2} \tag{34}$$

The error, introduced by calculating with equation (34) instead of the exact equation (14), is illustrated in figure 4. Here we see that for mild damping ($D_0 < 3.5$) and for $\varphi_0 > 3$ corresponding to the system constants of larger aircraft (ref. 1, p. 131), the error remains below 4 percent. For this reason we may calculate from here on without any objections with the approximation formula (34).

The characteristic chart of the following diagrams with linear damping are taken from the oft-mentioned prior report (ref. 1), whereby $\vartheta_1 = 0.2$ was chosen. Identical energy absorption assumes, according to equation (15), with equal shock velocity v_0 also equal maximum spring strokes, so long as $\lambda \neq 1$, that is, as long as the weight cancellation (by lift) is incomplete. With full weight cancellation ($\lambda = 1$), however, various comparison diagrams may be found with quadratic damping, as shown in figure 3. In the following, with full weight cancellation, identical maximum forces are presupposed.

When establishing that

$$\left.\begin{aligned} Q_{S_g} &= S_{g2}/S_{g1}, \qquad Q_{\psi_g} = \psi_{g2}/\psi_{g1}, \\ Q_{D_0} &= D_{02}/D_{01}, \qquad Q_\eta = \eta_2/\eta_1 \end{aligned}\right\} \tag{35}$$

wherein the subscript 1 relates to linear damping and subscript 2 to quadratic damping, figure 5 is given with a complete lack of weight cancellation, whereas figure 6 is given for full weight cancellation. The solid line curves relate to nonpreloaded spring struts and the broken line curves relate to a preloading equal to the static load.

Thus, for $\lambda = 0$, the spring strokes are identical for both damping laws, whereas in the practical region of φ_0 the maximum forces with quadratic damping are 5.5 to 7.5 percent lower than with linear damping. The springing effectiveness values η_2 are by 6 to 7.5 percent larger than the springing effectiveness values η_1.

With full weight cancellation ($\lambda = 1$, fig. 6) the maximum spring strokes ψ_{g2} are, for equal maximum forces, larger than the spring strokes ψ_{g1} by approximately 10 percent; whereas the springing effectiveness values are, with quadratic damping, on the average 10 percent below those with linear damping.

The initial damping D_{02} becomes at $\sigma = 1$ for $\varphi_0 = 1.48$, equal to zero (point a) so that the course of the curves for values $\varphi < 1.48$ has no more practical meaning. Thus the $Q\eta$-curve ends in point b. For smaller values of φ_0, a comparison is no more possible for known reasons (ref. 1); this is, however, of no consequence.

When, in conclusion, figs. 5 and 6 are viewed again, it may be seen that the realization of a quadratic damping law would offer no advantages over the linear damping. One should be therefore satisfied with the fact that in airplane struts with fluid damping the damping generally depends linearly on the spring compression velocity.

The next partial report, possibly even a third one, shall be devoted to the investigation of force-deflection diagrams with a nonlinear springing characteristic and linear or quadratic damping.

Translated by John Perl
Lockheed Aircraft Corp.

REFERENCES

1. Schlaefke, K.: Zum Vergleich von gepufferten und ungepufferten Federstössen an Flugzeugfahrwerken. Techn. Ber., Bd. 10, 1943, p. 129.

2. Schlaefke, K.: Zur Kenntnis der Wechselwirkungen zwischen Federbein und Reifen beim Landestoss von Flugzeugfahrwerken. Techn. Ber., Bd. 10, 1943, p. 363.

3. Klotter, K.: Einführung in die Technische Schwingungslehre. Bd. 1, Berlin 1938, p. 93.

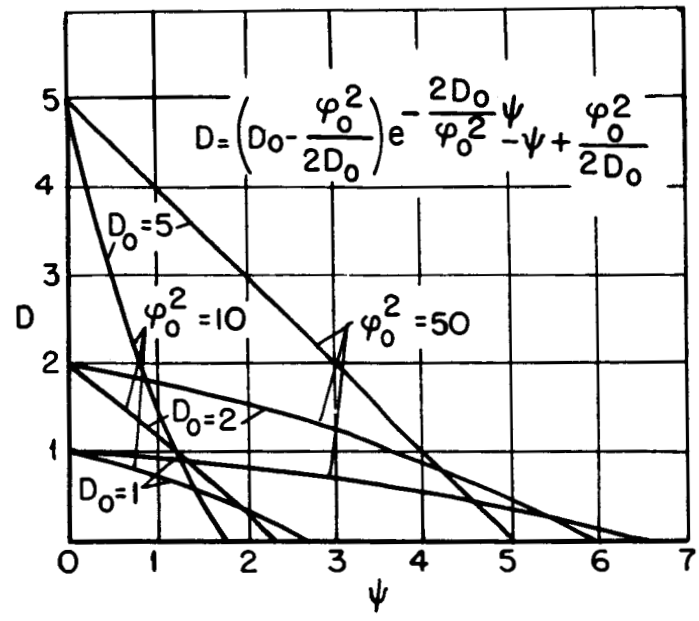

Figure 1.- Variation of the damping force as function of the spring stroke.

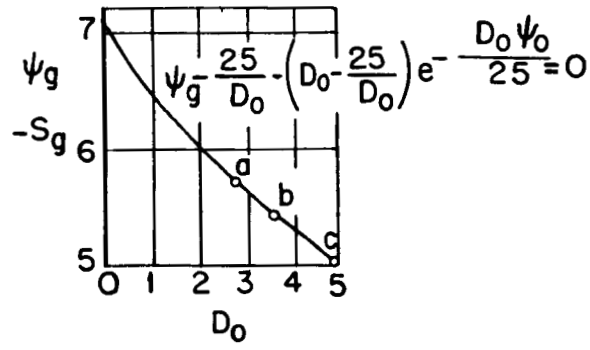

Figure 2.- Relationship between maximum spring stroke and initial damping (example).

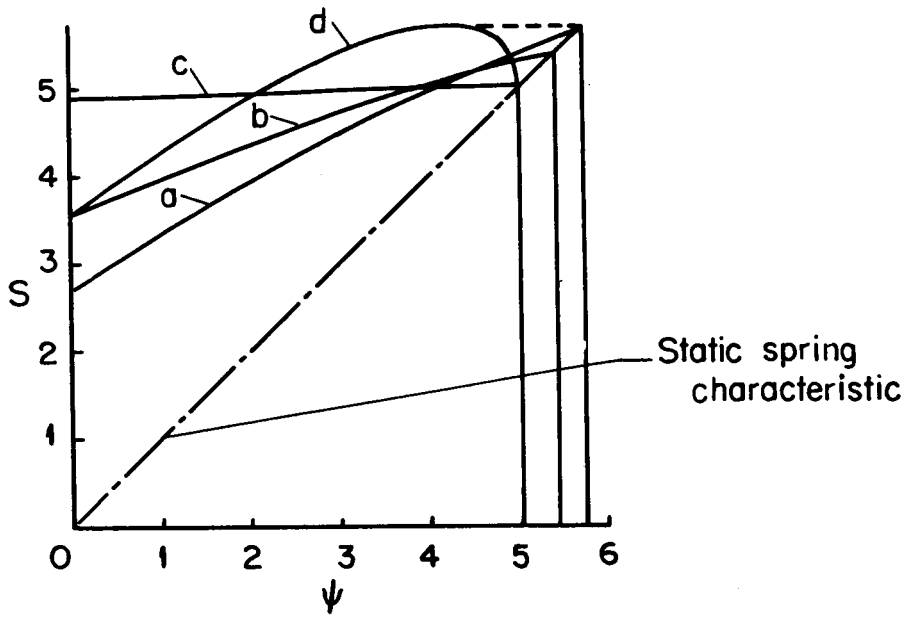

Figure 3.- Comparison of three diagrams of quadratic damping (a, b, and c), with a diagram of linear damping (d).

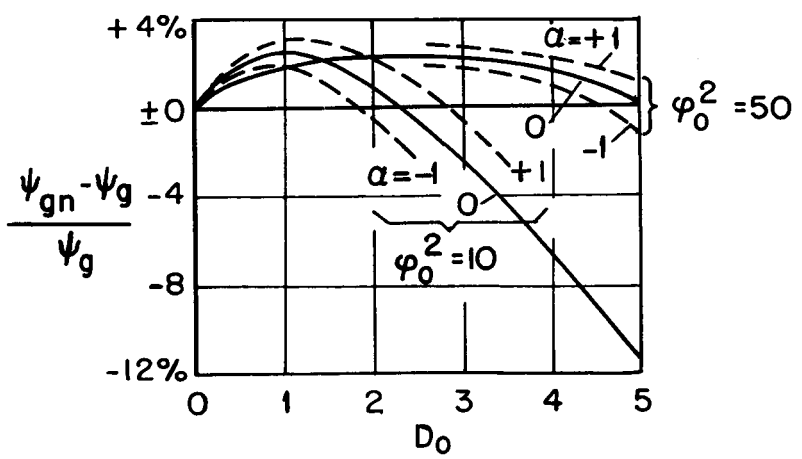

Figure 4.- Accuracy of the approximation formula 34 compared to the exact formula 14.

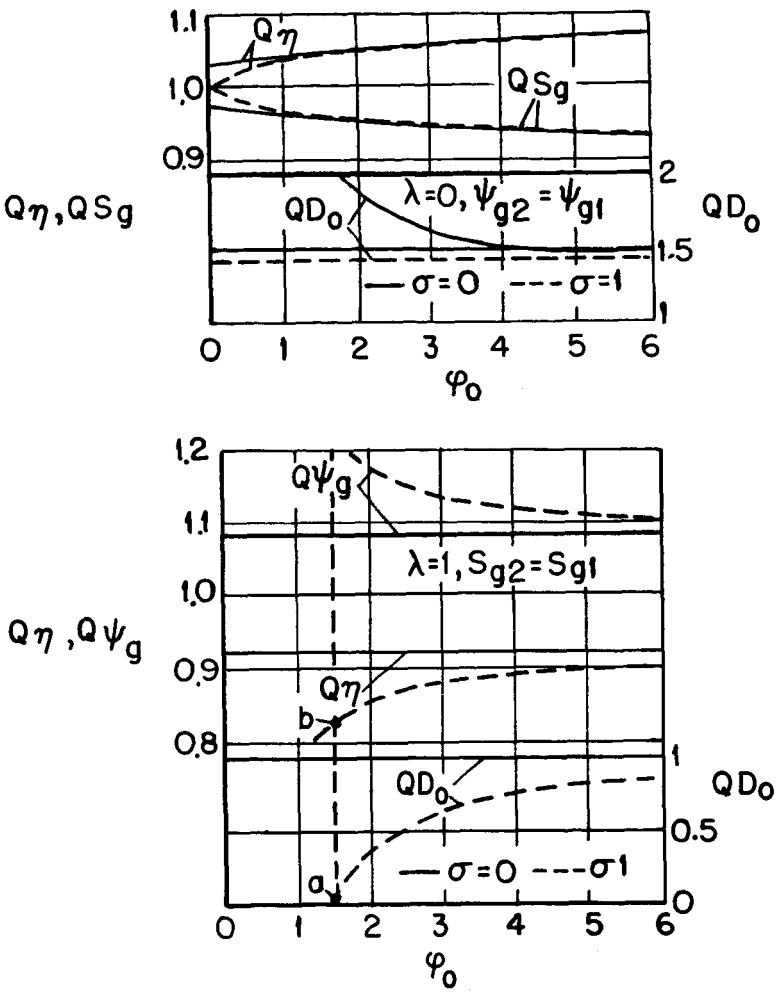

Figures 5 and 6.- Comparison of the maximum forces, greatest spring strokes, springing effectivenesses, and initial dampings with quadratic damping, with the same values in linear damping.

SECOND PARTIAL REPORT - APPROXIMATION METHOD FOR THE CALCULATION OF FORCE-DEFLECTION DIAGRAMS WITH A NONLINEAR SPRING CHARACTERISTIC AND LINEAR OR QUADRATIC DAMPING*

By K. Schlaefke

Summary: While undamped nonlinear oscillations on one hand, and damped harmonic oscillations on the other may be treated with mathematical exactness, one is dependent on an approximation method for the investigation of damped nonlinear oscillations. In the present report will be developed two approximation methods, their use described and critically examined.

Airplane shock-absorber struts, in their most employed form of air-spring struts with annular oil damping, represent oscillation elements with nonlinear spring characteristic and velocity-proportional damping. To the undamped nonlinear oscillations already a number of thorough investigations (refs. 1, 2, and 3) have been devoted. With the same thoroughness have been explained the damped harmonic oscillations (refs. 4, 5, and 6). In contrast thereto nothing as yet has been published on damped nonlinear oscillations that arise out of the combination of both above mentioned individual problems. The present investigation therefore deals with this naturally true oscillation problem. Whereby the promise, made at the conclusion of the first partial report (ref. 7), shall be fulfilled.

The calculation of damping-free nonlinear oscillations leads to elliptical integrals, whereas that of the damped harmonic oscillations leads to differential equations which cannot be solved quite simply. With this in both cases the limit is reached for exact mathematical solutions. For this reason it is easily understood that a combination of both problems remains from the start, not amenable to exact treatment. Yet the technical developments require data for construction and test. Thus we are confronted with the problem to find a useful approximation method for the calculation of force-deflection diagrams for the first landing shock of oil-air spring struts.

After a few preliminary trials I have decided on the method described below in which the force-deflection diagram is subdivided into a greater

---

*"Zur Kenntnis der Kraftwegdiagramme von Flugzeugfederbeinen, 2. Teilbericht: Näherungsverfahren zum Berechnen der Kraftwegdiagramme mit nichtlinearer Federkennlinie und linearer oder quadratischer Dämpfung." Technische Berichte, Bd. 11, Heft. 4, Apr. 25, 1944, pp. 105-109.

number of such small increments that the spring force as well as damping force in them may be considered as a straight line with the spring compression. Then from the energy-balance an equation may be easily derived for the step-by-step calculation of the diagram.

Figure 1 applies to linear and figure 2 to quadratic damping. The designations have been already discussed previously (ref. 5) so that at this time we shall, insofar as danger exists in confusing the linear with quadratic damping in their appearance side-by-side, designate the values with linear damping by the subscript 1, and those of quadratic damping with subscript 2. Then the energy balance for linear damping in decrement Δf_i is

$$\frac{M}{2}\left(v_{i-1}^2 - v_i^2\right) + Mg(1 - \lambda)\Delta f_i = \frac{P_{i-1} + P_i}{2}\Delta f_i$$

$$= \frac{P_{i-1} + F_i + k_1 v_i}{2}\Delta f_i \qquad (1)$$

From this equation is obtained

$$v_i = -\frac{k_1 \Delta f_i}{2M} + \sqrt{\left(\frac{k_1 \Delta f_i}{2M}\right)^2 + v_{i-1}^2 - \left(\frac{P_{i-1} + F_i}{M} - 2g(1 - \lambda)\right)\Delta f_i} \qquad (2)$$

This is already the formula for the step-by-step calculation of the force deflection diagram with an arbitrary spring chart approximated by interpolation and with linear damping. When a step leads to a complex numerical value of v_i, in which case the expression under the root becomes negative, calculation is to be made with the formula for the end section. The latter reads

$$\Delta f_n \approx \frac{\frac{M}{2} v_{n-1}^2}{\frac{P_{n-1} + F_{n-1}}{2} - Mg(1 - \lambda)}$$

$$= \frac{A - J_{n-1}}{\frac{P_{n-1} + F_{n-1}}{2} - Mg(1 - \lambda)} \qquad (3)$$

Herein it is approximatively assumed that the mean force P in the end section is equal to the arithmetic mean of P_{n-1} and F_{n-1}; this mean value is plotted in figures 1 and 2 with a dot and dash line. A designates the total work $\frac{M}{2} v_0^2$ and J_{n-1} denotes the energy absorbed by the spring strut up to the spring compression f_{n-1}.

The energy balance for quadratic damping (fig. 2) is as follows:

$$\frac{M}{2}\left(v_{i-1}^2 - v_i^2\right) + Mg(1 - \lambda)\Delta f_i = \frac{P_{i-1} + F_i + k_2 v_i^2}{2}\Delta f_i \tag{4}$$

From this is obtained

$$v_i = \sqrt{\frac{v_{i-1}^2 - \left(\frac{P_{i-1} + F_i}{M} - 2g(1 - \lambda)\right)\Delta f_i}{1 + \frac{k_2 \Delta f_i}{M}}} \tag{5}$$

The section-formula (3) is also valid for quadratic damping.

The application of the formulas shall be shown on an example. For the construction model Bf109B we have according to Kochanowsky (ref. 8)

$$\left.\begin{aligned} c &= 29000 \text{ kg/m} \\ M &= 100 \text{ kg s}^2/\text{m} \end{aligned}\right\} \tag{6}$$

With this is derived

$$\omega = \sqrt{\frac{c}{M}} = 17.0294 \text{ 1/s} \tag{7}$$

Furthermore we assume (fig. 3)

$$\left.\begin{aligned} F_0 &= 491 \text{ kg} \\ v_0 &= 4.2 \text{ m/s} \\ \vartheta_1 &= 0.25 \\ k_1 &= 2\sqrt{cM}\vartheta_1 = 851.5 \text{ kg s/m} \\ k_1 v_0 &= 3576 \text{ kg} \end{aligned}\right\} \tag{8}$$

A straight line characteristic chart was purposely assumed so that the diagram may be also calculated and thus the accuracy of the approximation method may be judged.

Thus is obtained for full weight cancellation ($\lambda = 1$) from the formulas of my prior report (ref. 5) the following

$$\left.\begin{aligned} f_g &= 0.1635 \text{ m} \\ f* &= 0.1380 \text{ m} \\ P_g &= 5960 \text{ kg} \end{aligned}\right\} \tag{9}$$

The approximation calculation was conducted from $f = 0$ to $f = 120$ mm in 6 steps of $\Delta f = 20$ mm according to the equation

$$v_i = -0.08515 + \sqrt{0.00725 + v_{i-1}^2 - 0.00020\left(P_{i-1} + F_i\right)} \tag{10}$$

with which numerical table 1 was obtained.

Since, at $f = 120$ mm, we have already approached toward the maximum force P, the steps following are reduced. From $f = 120$ mm on, calculation is then made with $\Delta f = 4$ mm according to the equation

$$v_i = -0.01703 + \sqrt{0.00029 + v_{i-1}^2 - 0.00004\left(P_{i-1} + F_i\right)} \tag{11}$$

The citation of the individual values is superfluous, since the calculation is made basically in the same manner as carried out in the numerical table 1.

For $f = 160$ mm is obtained $v = 0.755$ m/s. The step following leads to a negative value below the root sign of equation (11), so that we should calculate with the sectional formula (3) with

$$\left.\begin{aligned} A &= 882 \text{ mkg} \\ J_{n-1} &= 853.5 \text{ mkg} \\ P_{n-1} &= 5774 \text{ kg} \\ F_{n-1} &= 5130 \text{ kg} \end{aligned}\right\} \tag{12}$$

Then we obtain

$$\Delta f_n \approx \frac{882 - 853.5}{5452} = 0.0052 \text{ m} \tag{13}$$

and, consequently, $f_g = 0.1652$ m. Since, according to the discussed method, the maximum value of the force is given as $P_g = 6012$ kg (fig. 3),

the deviation of this from the true value according to equation (9) is +52 kg = +0.9 percent, whereas the error in the determination of the maximum spring stroke is +1.7 mm = +1.0 percent. In the example treated, the accuracy of the approximation method is therefore excellent, especially when considering that for its completion altogether only 17 steps were calculated for which, inclusive all side-calculations, not even one-half working day was required.

The approximation calculation with quadratic damping may be made still faster since in that case the damping curve shows an almost linear course. Beginning with the same initial damping as with linear damping, calculation is made from $f = 0$ to $f = 160$ mm in 8 steps with $K_2 = 202.7$ kg s^2/m^2 according to the formula

$$v_i = 0.98033 \sqrt{v_{i-1}^2 - 0.00020\left(P_{i-1} + F_i\right)} \tag{14}$$

Because the next step to $f = 180$ mm would lead to a negative value below the root sign, from $f = 160$ mm on we use, with

$$\left.\begin{aligned} A &= 882 \text{ mkg} \\ J_{n-1} &= 781.5 \text{ mkg} \\ P_{n-1} &= 5546 \text{ kg} \\ F_{n-1} &= 5130 \text{ kg} \end{aligned}\right\} \tag{15}$$

the end-section formula (3) from which is obtained

$$\Delta f_n \approx 0.0188 \text{ m} \tag{16}$$

Thus we have $f_g = 0.1788$ m and $P_g = 5676$ kg. In exact calculation one obtains from the equation (ref. 7, eq. (14))

$$\psi_g - 6.7914 - 3.1460\, e^{-0.1372\psi_g} = 0 \tag{17}$$

by trial and error, $\psi_g = 5.2629$; therefore,

$$f_g = 5.2629 \frac{g}{\omega^2} = 0.1780 \text{ m} \tag{18}$$

With this we obtain

$$P_g = 491 + 29000 \times 0.1780 = 5653 \text{ kg} \tag{19}$$

The approximation calculation for quadratic damping with an error of +0.8 mm = +0.45 percent in the maximum spring stroke and an error of +23 kg = +0.41 percent in the maximum force is, therefore, even more exact than for linear damping.

As a third example for the approximation calculation, a pneumatic spring strut with linear damping shall be investigated. Said calculation will employ the following basic values

$$\left.\begin{aligned} M &= 100 \text{ kg s}^2/\text{m} \\ F_0 &= 500 \text{ kg} \\ k &= 1000 \text{ kg s/m} \\ v_0 &= 3.8 \text{ m/s} \\ A &= 722 \text{ mkg} \end{aligned}\right\} \tag{20}$$

The equation for the compressive line reads (with f in mm)

$$F = F_0(1 - f/200)^{-1.3} \tag{21}$$

Again 6 steps of $\Delta f = 20$ mm are calculated from $f = 0$ to $f = 120$ mm according to the equation

$$v_i = -0.1 + \sqrt{0.01 + v_{i-1}^2 - 0.00020\left(P_{i-1} + F_i\right)} \tag{22}$$

and from here on, the succeeding steps with $\Delta f = 4$ mm are calculated according to the equation

$$v_i = -0.02 + \sqrt{0.0004 + v_{i-1}^2 - 0.00004\left(P_{i-1} + F_i\right)} \tag{23}$$

At $f_{n-1} = 172$ mm the residual calculation now sets in which leads to

$$\Delta f_n \approx \frac{722 - 719.7}{\frac{1}{2}(6709 + 6442)} = 0.00035 \text{ mm} \approx 0.4 \text{ mm} \tag{24}$$

Thus, we have $f_g = 172.4$ mm and $P_g = 6710$ kg. Of the total work A = 722 mkg, the airstrut absorbs 271 mkg = 37.5 percent while 451 mkg = 62.5 percent dissipated by the oil damping. This distribution markedly differs from that of figure 3; with a straight-line spring characteristic the spring absorbs here 53.1 percent of the total energy and the linear damping 46.9 percent.

In elaboration of these investigations, the spring compression time t_n is also to be determined, which elapses until attainment of the maximum loading deflection.

Generally the following expression applies

$$v = \frac{df}{dt} \quad \text{or} \quad dt = \frac{df}{v} \tag{25}$$

from which is had by integration

$$t_i = \int_0^{f_i} \frac{df}{v} \tag{26}$$

Since this expression becomes indetermined for $v = 0$, that is, for $f_i = f_n$, its value is found by step-by-step calculation to f_{n-1} and exclusive application of a residual formula.

To set up said residual formula, the law for the velocity course in the last increment must be known or must be assumed. Here is assumed that for linear, as well as quadratic damping, between f_{n-1} and f_n the velocity decreases per figure 5; this assumption will be more or less found to correspond to actuality. Then we have

$$\frac{1}{v} = \frac{1}{v_{n-1}} \sqrt{\frac{\Delta f_n}{f_n - f}} \tag{27}$$

and, with it

$$t_i = t_{n-1} + \int_{f_{n-1}}^{f_i} \frac{df}{v} = t_{n-1} + \frac{2\,\Delta f_n}{v_{n-1}} - \frac{2\sqrt{\Delta f_n (f_n - f_i)}}{v_{n-1}} \tag{28}$$

For $f_i = f_n$ is thus obtained

$$t_n = t_{n-1} + \frac{2\,\Delta f_n}{v_{n-1}} \tag{29}$$

The step-by-step calculation of the oscillation time, for the example per figure 3, with linear damping, yields $t_{n-1} = 0.0646$ s, so that with $\Delta f_n = 0.0052$ m and $\frac{1}{v_{n-1}} = 1.3238$ s/m, we obtain $t_n = 0.0784$ s. The

oscillation time t_n, however, is equal $T/4$ when T denotes the oscillation period. This is obtained as

$$T = \frac{2\pi}{\nu} = \frac{2\pi}{\omega} \frac{1}{\sqrt{1 - \vartheta_1^2}} = 0.3811 \text{ s} \tag{30}$$

whereas $4t_n = 0.3136$ s. Thus, the value is by 0.0675 s = 17.7 percent below the true value.

For quadratic damping an error is found of a similar magnitude. According to Klotter (ref. 1, p. 95) the oscillation period at quadratic damping is nearly equal to that with complete absence of damping

$$T \approx \frac{2\pi}{\omega} = 0.3685 \text{ s} \tag{31}$$

In the step-by-step calculation of the time intervals, we arrive at $t_{n-1} = 0.0561$ s so that, with $\Delta f_n = 0.0188$ m and $\frac{1}{v_{n-1}} = 0.6982$ s/m, we obtain $t_n = 0.0823$ s. Thus we have here also $4t_n = 0.3292$ s which is, by 10.7 percent of the correct value, too small.

Although the time determination was made with the greatest care, the results are unusable. The time may be calculated with sufficient accuracy then only when the velocity as a function of the spring stroke is given as a mathematical expression. Arbitrary assumptions will also lead to great errors even when the assumptions depart very slightly from reality.

In general, the time is of little interest in drop testing of airplane shock struts so that the failure of calculations may not be decried. This question was aired here for the sole purpose to show that further activities in this field may be pronounced in advance as futile.

The above treated examples point, with closer scrutiny, to a second method of approximative calculation of drop tests on which shall be reported below. Namely, when plotting the dimensionless form v/v_0 as a function of f/f_g we obtain (see fig. 6) for the linear spring chart and linear damping curve according to figure 3, in solid lines, and for the nonlinear case the broken line curve, shown in figure 4. Both curves run so close together that an attempt was made to replace them with a single curve and to give the latter general validity. The approximation curve of the course of the dot-and-dash line follows the law as shown below.

$$v = v_0\sqrt{1 - f/f_g} \tag{32}$$

At first we shall investigate under what condition the above law of equation (32) is truly fulfilled. The attempt, by series expansion of the ln and arc tan expression of the exact solution, to interpret equation (32) for a linear spring characteristic and linear damping (see ref. 5, p. 130, eq. (12)) had completely failed. (Translator's remark: Due to a missing comma, the German sentence is difficult of interpretation. We have done our best in translating the involved sentence, but recommend caution in accepting it.) When considering only the first member in both of the series, one already arrives at an equation of the 3rd degree between v and f, with which nothing can be undertaken. Irrespective of same, the series development for the arc tan expressions is unreliable from the start since, per example for $\alpha = 0$ and $\vartheta = 0.25$, the value $\frac{\varphi_0\sqrt{1 - \vartheta^2}}{\vartheta\varphi_0 - \alpha} = 3.87$ is essentially greater than 1.

A second attempt for solving equation (32) starts out with the differential equation. (See ref. 5, p. 130, eq. (3).)

$$\frac{d\varphi}{d\psi} + \frac{\psi - \alpha}{\varphi} + 2\vartheta = 0 \tag{33}$$

When now making the assumption which, at first appears quite arbitrary, that

$$\vartheta = \frac{1}{2\sqrt{2}}\frac{\varphi}{\varphi_0} \tag{34}$$

that is, calculating with a direct proportionality between ϑ and φ and assuming that the value $\vartheta = 0.25$ is attained at the mean ratio $\varphi/\varphi_0 = \frac{1}{2}\sqrt{2}$, then this assumption, although distasteful to the mathematical expert, should nevertheless offer no great practical errors for medium values of ϑ:

Equation (33) written with (34) gives

$$\frac{d\varphi}{d\psi} + \frac{\psi - \alpha}{\varphi} + \frac{1}{\sqrt{2}}\frac{\varphi}{\varphi_0} = 0 \tag{35}$$

when inserting into this equation

$$\varphi = \varphi_0\sqrt{1 - \psi/\psi_g} \tag{36}$$

and its differential quotient

$$\frac{d\varphi}{d\psi} = -\frac{\varphi_0}{2\psi_g}\frac{1}{\sqrt{1 - \psi/\psi_g}} = -\frac{\varphi_0^2}{2\varphi\psi_g} \tag{37}$$

we thus obtain

$$-\frac{\psi_0^2}{2\psi_g} + \psi - \alpha + \frac{\varphi_0}{\sqrt{2}}\left(\frac{\varphi}{\varphi_0}\right)^2 = 0 \tag{38}$$

For $\varphi = 0$ we have $\psi = \psi_g$; therefore,

$$-\frac{\varphi_0^2}{2\psi_g} + \psi_g - \alpha = 0 \tag{39}$$

or

$$\psi_g = \frac{\alpha}{2} + \sqrt{\frac{\varphi_0^2}{2} + \left(\frac{\alpha}{2}\right)^2} \tag{40}$$

When inserting equation (39) into (38) we obtain

$$-\psi_g + \psi + \frac{\varphi_0}{\sqrt{2}}\left(\frac{\varphi}{\varphi_0}\right)^2 = 0 \tag{41}$$

Furthermore, since according to equation (39)

$$\frac{\varphi_0}{\sqrt{2}} = \psi_g\sqrt{1 - \frac{\alpha}{\psi_g}} \approx \psi_g \tag{42}$$

we obtain finally

$$-1 + \psi/\psi_g + (\varphi/\varphi_0)^2 = 0 \tag{43}$$

or

$$\varphi = \varphi_0\sqrt{1 - \psi/\psi_g} \tag{44}$$

This is the assumed velocity course per (32) or (36). With this we again return to equation (32). When assuming generally such velocity course with the compression of the spring strut, a second method is obtained for

the approximative calculation of the force-deflection diagrams. For a linear spring characteristic and linear damping with equation (32) we have

$$P = F_0 + cf + kv_0\sqrt{1 - f/f_g} \tag{45}$$

By setting the differential quotient to zero, one obtains

$$\frac{dP}{df} = 0 = c - \frac{kv_0}{2f_g}\frac{1}{\sqrt{1 - f_*/f_g}} \tag{46}$$

or

$$f_* = f_g\left(1 - \left(\frac{kv_0}{2f_g c}\right)^2\right) \tag{47}$$

When inserting this expression into equation (45), we obtain

$$P_g = F_0 + cf_g + \frac{k^2 v_0^2}{4f_g c} \tag{48}$$

or, in the form written per my former report (ref. 5)

$$S_g = \sigma + \psi_g + \frac{\vartheta^2 \varphi_0^2}{\psi_g} \tag{49}$$

The maximum value of the spring deflection f_g is determined from the energy balance. First we obtain with $x = f/f_g$

$$\int_0^{f_g} kv\,df = kv_0 f_g \int_0^1 \sqrt{1 - x}\,dx = \frac{2}{3} kv_0 f_g \tag{50}$$

This implies that the mean velocity v_m between $f = 0$ and $f = f_g$ is equal $\frac{2}{3} v_0$. With

$$\left.\begin{aligned} J_F &= F_0 f_g + \frac{cf_g^2}{2} \\ J_D &= \frac{2}{3} kv_0 f_g \end{aligned}\right\} \tag{51}$$

is, furthermore

$$J_F + J_D = \frac{M}{2} v_0^2 + (Mg - L)f_g \tag{52}$$

When combining the two last equations we obtain

$$f_g^2 + 2f_g \frac{\frac{2}{3} kv_0 - (Mg - L - F_0)}{c} - \left(\frac{v_0}{\omega}\right)^2 = 0 \tag{53}$$

and finally

$$f_g = -\frac{\frac{2}{3} kv_0 - (Mg - L - F_0)}{c} + \sqrt{\left(\frac{v_0}{\omega}\right)^2 + \left(\frac{\frac{2}{3} kv_0 - (Mg - L - F_0)}{c}\right)^2} \tag{54}$$

Written in a different form, equation (54) reads

$$\psi_g = -\left(\frac{4}{3} \vartheta\varphi_0 - \alpha\right) + \sqrt{\varphi_0^2 + \left(\frac{4}{3} \vartheta\varphi_0 - \alpha\right)^2} \tag{55}$$

When calculating the approximate values S_g by equation (49) and ψ_g by equation (55), and comparing them with the exact values (ref. 5, p. 130, eqs. (13a) and (20)), it is found that with freedom from damping ($\vartheta = 0$) both values show perfect agreement. For $\vartheta = 0.2$ and 0.4 figures 7 and 8 apply. It may be seen that for $\alpha = 0$ and $\alpha = -1$, that is, for $1 \leqq \lambda + \sigma \leqq 2$, corresponding to the actual conditions with $\sigma \approx 0.5$ and $\lambda = 1$, the errors of S_g and ψ_g remained below 1 percent, and in the spring stroke determination for $\alpha = 0$ and $\vartheta = 0.2$ only rose to 1.6 percent. For $\alpha = 1$, the errors increase with decreasing φ_0, which regions, however, are practically meaningless since, in the first place the spring struts are always preloaded, and secondly, φ_0 hardly ever is smaller than 3 (ref. 5, p. 131, left column).

Thus, calculations may be made with the second approximation method at least as long as more exhaustive test results from experts will place the once-for-all necessary preliminary calculations of oil-air spring struts on fully reliable foundations.

In the next partial report the here obtained results shall be used in order to gain a general perspective on the maximum forces, maximum spring deflections and spring capacities occurring in the landing shocks of oil-air spring struts.

Translated by John Perl
Lockheed Aircraft Corp.

REFERENCES

1. Klotter, K.: Einführung in die Technische Schwingungslehre. Bd. 1, Berlin 1938, p. 98ff.

2. Weigand, A.: Zur Theorie der Fahrzeugfederung, insbesondere der progressiven Federung. Forsch. Ing.-Wes., Bd. 11, 1940, p. 309.

3. Weigand, A.: Die Berechnung freier nichtlinearer Schwingungen mit Hilfe der elliptschen Funktionen. Forsch. Ing.-Wes., Bd. 12, 1941, p. 274.

4. Michael, F.: Theoretische und experimentelle Grundlagen für die Untersuchung und Entwicklung von Flugzeugfederungen. Luftfahrtforsch, Bd. 14, 1937, p. 387. (Reprint of FB 87, 1934.)

5. Schlaefke, K.: Zum Vergleich von gepufferten und ungepufferten Federstössen an Flugzeugfahrwerken. Techn. Ber., Bd. 10, 1943, p. 129.

6. Schlaefke, K.: Zur Kenntnis der Wechselwirkungen zwischen Federbein und Reifen beim Landestoss von Flugzeugfahrwerken. Techn. Ber., Bd. 10, 1943, p. 363.

7. Schlaefke, K.: Zur Kenntnis der Kraftwegdiagramme von Flugzeugfederbeinen. 1. Teilbericht: Vergleich von Diagrammen mit linearer und quadratischer Dämpfung. Techn. Ber., Bd. 11, 1944, p. 51. (Presented in this translation as First Partial Report.)

8. Kochanowsky, W.: Landestoss und Rollstoss von Fahrwerken mit Ringfederbeinen. FB 1757, 1943.

TABLE I

EXAMPLE OF AN APPROXIMATION CALCULATION

f mm	F kg	v m/s	$k_1 v$ kg	P kg	J mkg
0	491	4.2	3,576	4,067	0
20	1,071	3.992	3,399	4,470	85.4
40	1,651	3.751	3,194	4,845	178.5
60	2,231	3.473	2,957	5,188	278.8
80	2,811	3.151	2,683	5,494	385.6
100	3,391	2.771	2,360	5,751	498.1
120	3,971	2.311	1,968	5,939	615.0

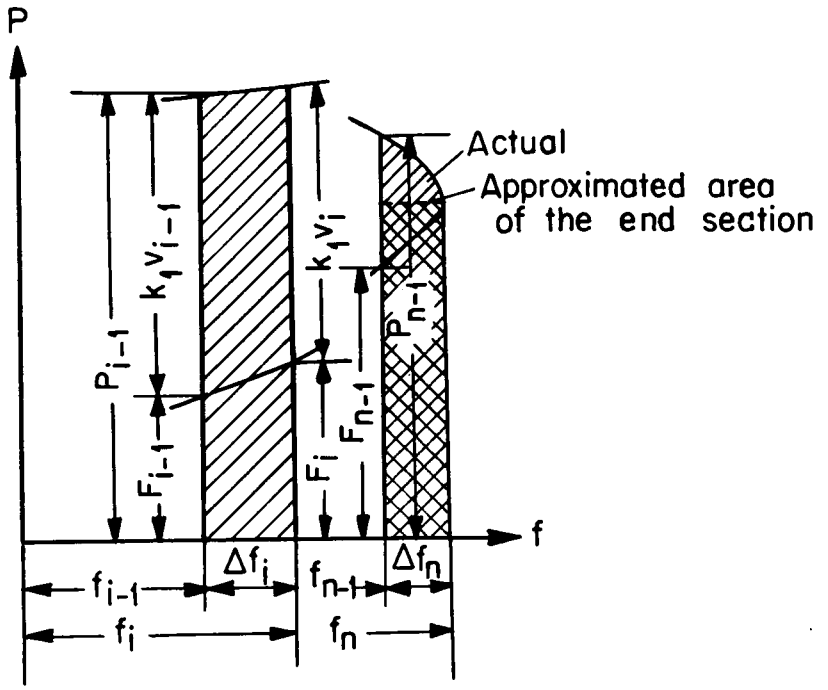

Figure 1.- Cutout of the force-deflection diagram between f_{i-1} and f_i and end-cutout between f_{n-1} and f_n (linear damping).

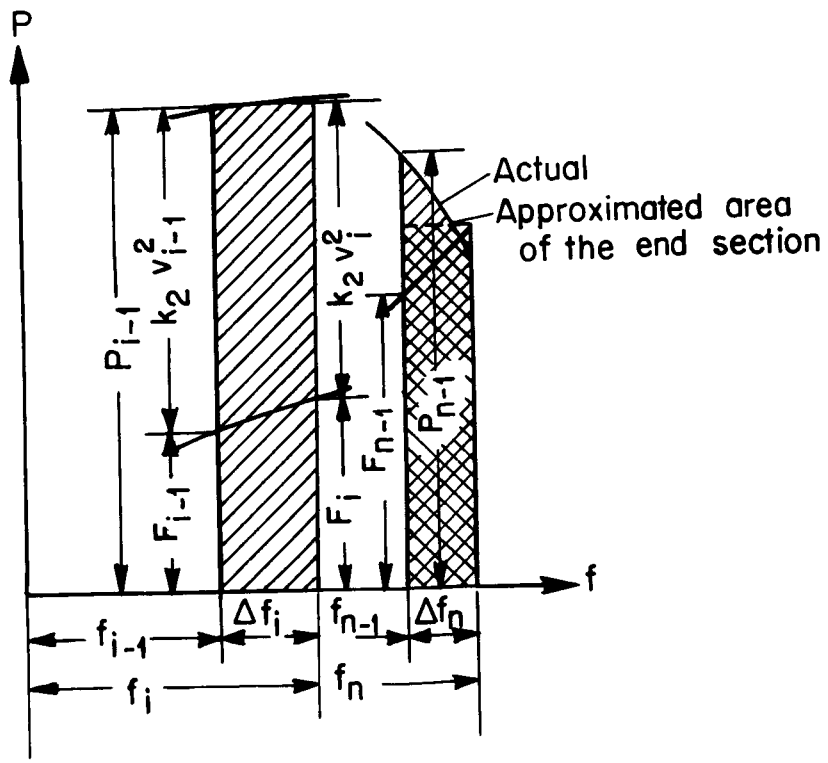

Figure 2.- Cutout of the force-deflection diagram between f_{i-1} and f_i and end-cutout between f_{n-1} and f_n (quadratic damping).

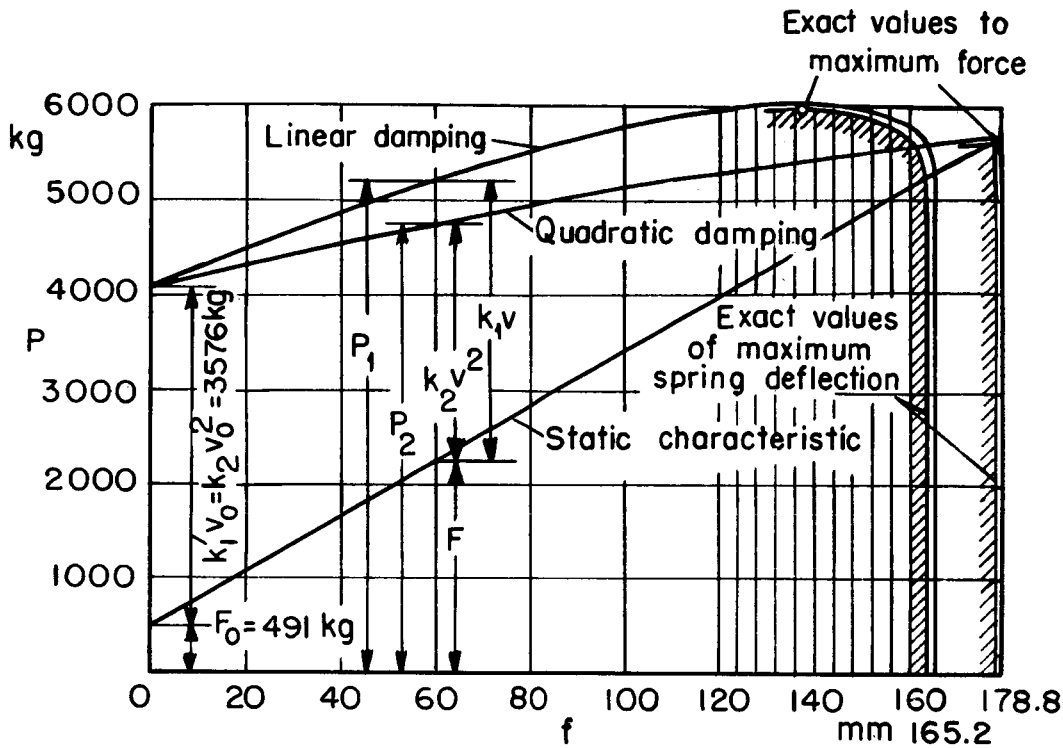

Figure 3.- Example of the step-by-step calculation of the force-distance diagrams with linear and quadratic damping.

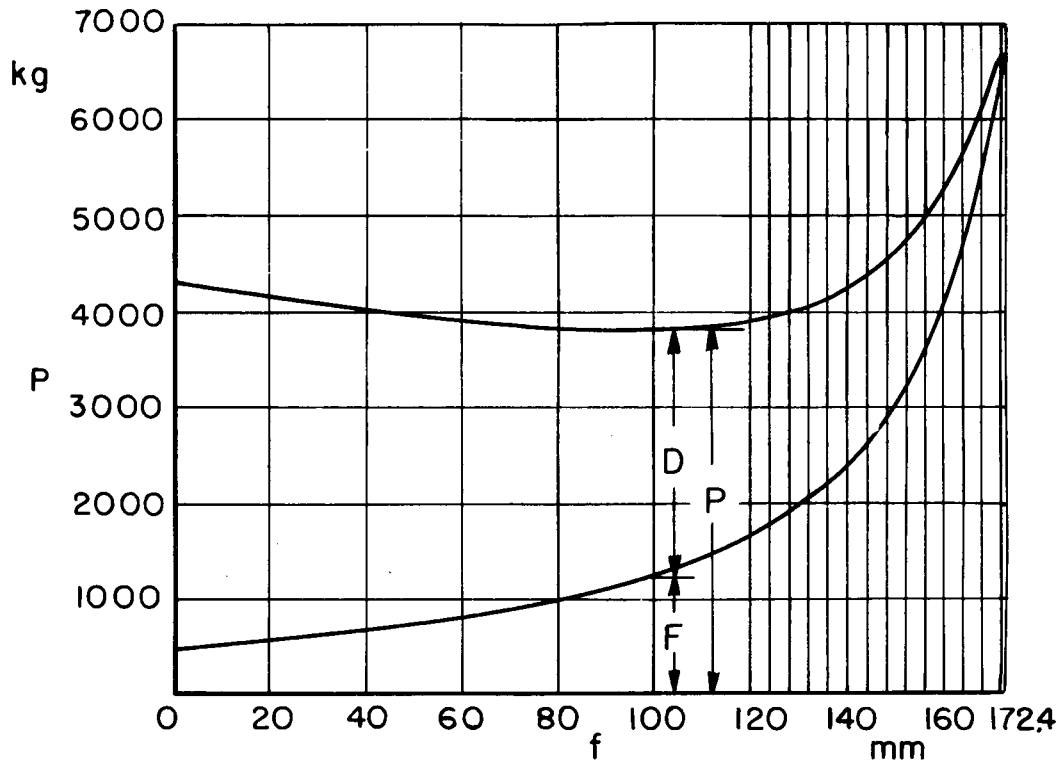

Figure 4.- Example for the step-by-step calculation of a force-deflection diagram with an undetermined spring chart and velocity-proportional damping. Oil-air strut.

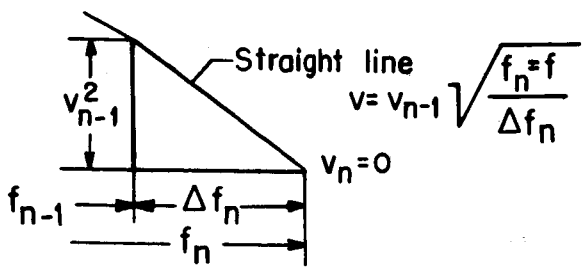

Figure 5.- Approximation calculation of the last time-period.

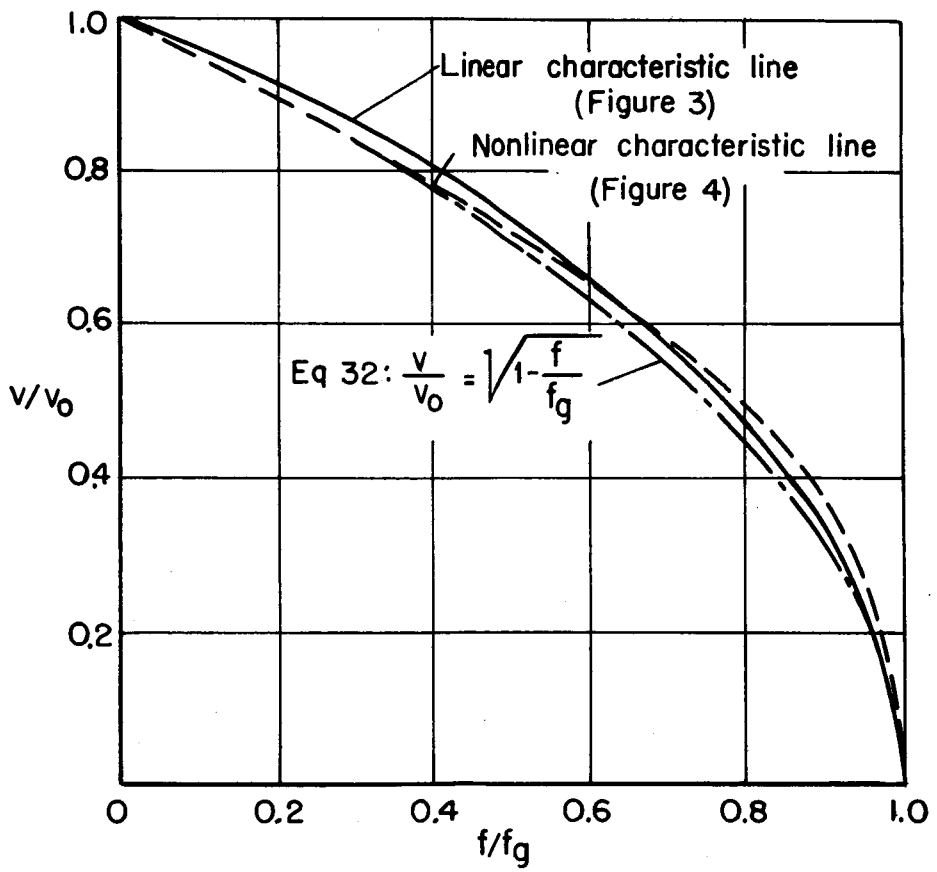

Figure 6.- Course of the spring compression velocity in function with the spring stroke.

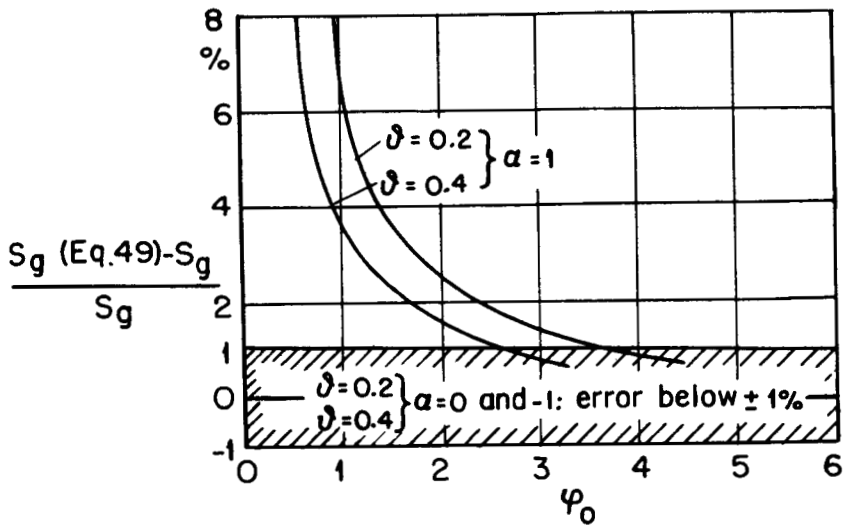

Figure 7.- Exactness of the approximation formula (equ. 55) for determination of ψ_g.

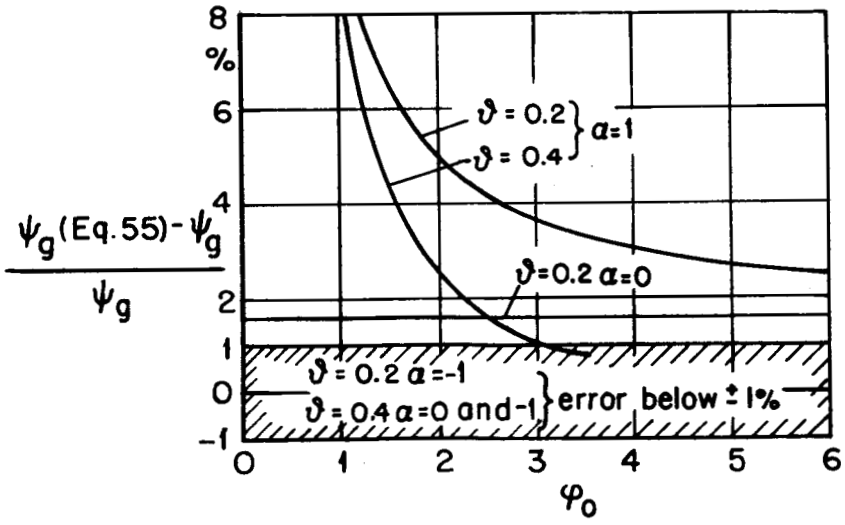

Figure 8.- Exactness of the approximation formula (equ. 49) for determination of S_g.

THIRD PARTIAL REPORT - THE LANDING IMPACT OF OLEO-PNEUMATIC SHOCK ABSORBERS*

By K. Schlaefke

Summary: The stress-stroke diagram of an oleo-pneumatic leg under the first impact at landing can be obtained by superposing onto the diagram of the undamped compressed-air leg, the damping diagram according to the second approximate method described in the preceding partial report (ref. 1). The maximum stroke, maximum load, and efficiency to be expected for various damping, lift coefficients, and heights of drop are computed and represented diagrammatically for practical use. Lastly, it is indicated how the newly introduced damping factor for oleo-pneumatic legs can be determined by experiment.

The present report may be joined to the second partial report (ref. 1) without further introduction. First to be considered is the compressed-air strut without damping, a problem which, in view of the generally known principles of thermodynamics, presents no difficulties.

The natural frequency ω has proved itself useful as characteristic value of linear spring systems because it enables the investigations to be represented in generally applicable dimensionless form. But, since ω is not a constant for nonlinear systems, a different characteristic value must be looked for. As such, the theoretical maximum spring travel or stroke f_0 appears to be the most suitable for oleo-pneumatic struts. It is the theoretical stroke required to raise the force F from the initial tension F_0 to $F = \infty$. On actually constructed struts f_0 ranges from 230 to 600 millimeters if one assumes, besides the limits indicated by Michael (ref. 2), $f_g/f_0 \approx 0.75$ for the maximum travel f_g.

The compression curve follows the law

$$F(f_0 - f)^k = F_0 f_0^k \qquad (1)$$

*"Zur Kenntnis der Kraftwegdiagramme von Flugzeugfederbeinen, 3. Teilbericht: Der Landestoss von Ölluftfederbeinen." Technische Berichte, Bd. 11, Heft. 5, May 15, 1944, pp. 137-141.

with

$$\frac{F}{Mg} = S_F \qquad \frac{F_0}{Mg} = \sigma \qquad \frac{f}{f_0} = \psi \tag{2}$$

equation (1) becomes

$$S_F = \sigma(1 - \psi)^{-k} = \sigma\Phi_1 \tag{3}$$

The energy absorbed by the compressed-air spring is

$$\int_0^{\psi} S_F d\psi = \sigma \frac{(1 - \psi)^{-(k-1)} - 1}{k - 1} = \sigma\Phi_2 \tag{4}$$

the rise of the compression curve

$$\frac{dS_F}{d\psi} = \sigma k(1 - \psi)^{-(k+1)} = \sigma\Phi_3 \tag{5}$$

The variation of the polytropic curve (fig. 1) should not be much different from that of the adiabatic curve because the landing impact is generally too fast for any appreciable heat flow. In the following, $k = 1.3$ is assumed, which incidentally is the same figure used by Irmer (ref. 3) and Hadekel (ref. 4) on the basis of experiments.

With $k = 1.3$, table 1 and figure 2 are obtained for the functions Φ_1, Φ_2, and Φ_3, in equations (3) to (5) with respect to ψ. It should be noted that the expansion of, for example, Φ_1 in series

$$\Phi_1 = (1 - \psi)^{-1.3} = 1 + 1.3\psi + 1.495\psi^2 + 1.6445\psi^3 + \ldots \tag{6}$$

is useless because this series converges very slowly for practical values of ψ. For $\psi = 0.5$ the error of the series value when breaking off after the term of third degree is already almost 10 percent, while for $\psi = 0.8$ the value still amounts to less than half of the correct value.

The compression f_r under static load is obtained from the equation

$$Mg(f_0 - f_r)^{1.3} = F_0 f_0^{1.3} \tag{7}$$

at

$$f_r/f_0 = \psi_r = 1 - \sigma^{1/1.3} \tag{8}$$

The relationship between ψ_r and σ is shown in figure 3. According to Hadekel (ref. 4) f_g/f_0 is mostly equal to 0.75 and $f_r/f_g = 0.5$ to 0.667; hence $\psi_r = 0.375$ to 0.5 and $\sigma = 0.40$ to 0.54 according to equation (8) or figure 3. In the following $\sigma = 0.5$ is used. This is in full agreement with Michael (ref. 2) who puts $S_{Fg} = 2.2$ to 3.5, while table 1 gives $S_{Fg} = 3.03$ for $\sigma = 0.5$ and $f_g/f_0 = 0.75$.

The energy balance for the landing impact of the undamped compressed-air leg ($\delta = 0$) reads

$$\int_0^{f_g} F \, df = Mg(H + (1 - \lambda)f_g) \tag{9}$$

or, in dimensionless form

$$A_F = \int_0^{\psi_g} S_F \, d\psi = \frac{H}{f_0} + (1 - \lambda)\psi_g \tag{10}$$

From the last equation follows

$$\left(H/f_0\right)_{\delta=0} = \sigma \frac{\left(1 - \psi_g\right)^{-0.3} - 1}{0.3} - (1 - \lambda)\psi_g \tag{11}$$

Equation (11) can be solved only for $\lambda = 1$ with respect to ψ_g. Therefore, it is better to simply consider ψ_g as independent and H/f_0 as dependent variable (table 1, columns 5 and 6). For round values of H/f_0 the corresponding values of ψ_g are obtained by interpolation. Incidentally, it should be noted that the maximum travel for the undamped spring impact ($\lambda = 0$) and $H = 0$ is $\psi_g = 0.68066$, a phenomenon already explained elsewhere (ref. 5).

The efficiency η for the pure compressed-air leg is

$$\eta = \frac{\left(1 - \psi_g\right)^{-0.3} - 1}{0.3\psi_g\left(1 - \psi_g\right)^{-1.3}} = \frac{\left(1 - \psi_g\right) - \left(1 - \psi_g\right)^{1.3}}{0.3\psi_g} \tag{12}$$

by which equation column 7 of table 1 was computed.

This concludes the study of the undamped compressed-air leg.

TABLE 1.- FUNCTIONS FOR COMPUTING THE COMPRESSION CURVE

1	2	3	4	5	6	7
ψ	Φ_1	Φ_2	Φ_3	(H/f_0) $\delta = 0,\ \lambda = 0$	(H/f_0) $\delta = 0,\ \lambda = 1$	η
0	1	0	1.3	0	0	1
0.1	1.1468	0.1070	1.6564	-0.0465	0.0535	0.933
0.2	1.3365	0.2306	2.1719	-0.0847	0.1153	0.863
0.3	1.5899	0.3764	2.9527	-0.1118	0.1882	0.789
0.4	1.9427	0.5520	4.2091	-0.1240	0.2760	0.711
0.5	2.4623	0.7704	6.4020	-0.1148	0.3852	0.626
0.55	2.8237	0.9024	8.1575	-0.0988	0.4512	0.582
0.6	3.2910	1.0546	10.696	-0.0727	0.5273	0.534
0.65	3.9149	1.2340	14.541	-0.0330	0.6170	0.485
0.7	4.7835	1.4500	20.729	0.0250	0.7250	0.433
0.725	5.3563	1.5766	25.321	0.0633	0.7883	0.406
0.75	6.0629	1.7190	31.528	0.1095	0.8595	0.378
0.775	6.9528	1.8814	40.173	0.1657	0.9407	0.349
0.8	8.1033	2.0690	52.671	0.2345	1.0345	0.320
0.825	9.6394	2.2896	71.607	0.3198	1.1448	0.288
0.85	11.7783	2.5556	102.08	0.4278	1.2778	0.255
0.875	14.9285	2.8670	155.26	0.5585	1.4335	0.219
0.9	19.9526	3.3176	259.39	0.7588	1.6588	0.185
0.925	29.0015	3.9170	502.70	1.0335	1.9585	0.146
0.95	49.1291	4.8550	1277.4	1.4775	2.4275	0.104
0.975	120.970	6.7476	6290.4	2.3988	3.3738	0.057
1	∞	∞	∞	∞	∞	0

The force-deflection diagram of the oleo shock absorber is obtained by superposing the damping diagram on the static diagram of the pneumatic shock absorber.

The damping force D proportional to the velocity follows in good approximation the law

$$D = D_0\sqrt{1 - f/f_g} \tag{13}$$

as proved in the previous partial report (ref. 1, equation 32, and fig. 6).

With a view to employing the characteristic value f_0 for characterizing the damping also, D_{f_0} is defined as the damping force that occurs in a landing impact from a drop of height f_0

$$D_{f_0} = k\sqrt{2gf_0} \tag{14}$$

Furthermore, since

$$D_0 = k\sqrt{2H} \tag{15}$$

the elimination of k from equations (14) and (15) together with equation (13) leaves

$$D = D_{f_0}\sqrt{H/f_0}\ \sqrt{1 - f/f_g} \tag{16}$$

or, with

$$\frac{D}{Mg} = S_D \qquad \frac{D_{f_0}}{Mg} = \delta \tag{17}$$

in dimensionless form

$$S_D = \delta\sqrt{H/f_0}\sqrt{1 - \psi/\psi_g} \tag{18}$$

According to the second partial report (ref. 1, equation (50))

$$A_D = \int_0^{\psi_g} S_D \, d\psi = \frac{2}{3} \delta \sqrt{H/f_0} \psi_g \tag{19}$$

with which the energy balance that serves for defining ψ_g becomes

$$A_F + A_D = \sigma \frac{(1 - \psi_g)^{-0.3} - 1}{0.3} + \frac{2}{3} \delta \sqrt{H/f_0} \psi_g = \frac{H}{f_0} + (1 - \lambda)\psi_g \tag{20}$$

For the numerical calculation, equation (20) is best solved with respect to H/f_0 as unknown. By equation (11)

$$\frac{H}{f_0} = \left[\frac{\delta \psi_g}{3} \pm \sqrt{\left(\frac{H}{f_0}\right)_{\delta=0} + \left(\frac{\delta \psi_g}{3}\right)^2} \right]^2 \tag{21}$$

The root disappears for the values of δ and ψ_g given in table 2.

TABLE 2

EVALUATION OF EQUATION (21)

δ	ψ_g	H/f_0	Figure 4
1.5	0.5805	0.0842	Point A
3	0.3456	0.1194	Point B

The curves have horizontal tangents in the two points A and B (fig. 4). But it is to be assumed that here the approximate calculation does not agree with reality; at any rate, there is no physical explanation for this variation of the curve. However, since such small values of H/f_0 are practically of no significance, the bare hint at the limits of the approximate calculation should be sufficient.

Thus, equation (21) is represented in figure 4 with the reservation that the anticipated maximum compression can be read off in terms of δ, λ, and H/f_0.

In figure 5, the maximum compression for free-drop and weight-balanced impact are compared; then $Q(\psi_g) = \psi_{g(\lambda=1)}/\psi_{g(\lambda=0)}$. Figure 5 similarly serves for defining the compression with weight-balanced impact from the experimental values of the free-drop impact, as explained in reference 5 for linear spring characteristic curves.

Before proceeding to the calculation of the maximum force, the limits of H/f_0 and δ up to which the calculation must be carried out so as to include the partial range, are determined.

It has been established that f_0 ranges between 230 and 600 millimeters. In the drop test the maximum height of drop H is about 1000 millimeters, equivalent to a maximum rate of drop $v_0 = 4.43$ meters per second. Thus H/f_0 is at the most equal to 1.67 for large aircraft and rises to a little more than 4 for small airplanes. Consequently, it is sufficient to extend the calculation to $H/f_0 = 4$, as already done in the evaluation of equation (21) in figure 4.

To define the average damping factor δ to be expected, recourse is had to the damping magnitude for linear spring characteristic curves, which as a rule lie at $\vartheta = 0.25$ (ref. 6).

Equating the two initial dampings, the equation

$$2\vartheta\varphi_0 = \frac{2\vartheta v_0 \omega}{g} = 2\vartheta\sqrt{H/f_g}\sqrt{2n} = \delta\sqrt{H/f_0} \tag{22}$$

with $n = 2.2$ to 3.5 (ref. 2, p. 395) and $f_g/f_0 = 0.75$ gives

$$\delta = \frac{0.5\sqrt{4.4}}{\sqrt{0.75}} \text{ to } \frac{0.5\sqrt{7}}{\sqrt{0.75}} = 1.2 \text{ to } 1.5 \tag{23}$$

Accordingly, the calculation was made with $\delta = 0$, $\delta = 1.5$, and $\delta = 3$, which surely includes the practical flight range.

The maximum force S_g is obtained by differentiating the equation

$$S = S_F + S_D = \sigma(1 - \psi)^{-1.3} + \delta\sqrt{H/f_0}\sqrt{1 - \psi/\psi_g} \tag{24}$$

with respect to ψ and putting the differential quotient equal to zero. Hence

$$\frac{\psi_g\left(1 - \psi_*/\psi_g\right)^{0.5}}{\left(1 - \psi_g\psi_*/\psi_g\right)^{2.3}} = \frac{\delta\sqrt{H/f_0}}{2.6\sigma} \tag{25}$$

This equation must be solved by trial. It is best to assume ψ_*/ψ_g as independent and δ as dependent variable, and ultimately define the applicable value of ψ_*/ψ_g for the correct value δ by interpolation. For $H/f_0 = 1.5$, $\lambda = 1$, $\sigma = 0.5$, and $\psi_g = 0.676$, a table such as table 3 is obtained. Interpolation for $\delta = 1.5$ results in

$$\left.\begin{aligned} \psi_*/\psi_g &= 0.9668 \\ \psi_* &= 0.6536 \\ S_g &= 2.319 \end{aligned}\right\} \tag{26}$$

TABLE 3

EXAMPLE FOR SOLVING EQUATION (25)

ψ_*/ψ_g =	0.96	0.97	0.98
δ =	1.594	1.444	1.234

Figure 6 represents the drop diagrams for several values of H/f_0 for $\delta = 1.5$ and complete lift relaxation, that is $\lambda = 1$. The point defined by equation (26) is indicated by the letter A. It is seen that the maximum value formation starts expressly between $H/f_0 = 1$ and $H/f_0 = 1.5$, but that this maximum exceeds the initial force only when H/f_0 still has risen a little above 1.5.

This is clearer yet in figure 7. The parabolas starting in the point with the coordinates $H/f_0 = 0$, $S_g = 0.5$ represent the initial forces. For $\delta = 1.5$ and $\lambda = 1$ the steeply rising branch is valid

from $H/f_0 = 1.53$ on. For such marked damping as $\delta = 3$ the maximum force for the weight-balanced impact in the entire range in question is equal to the initial force, while for the undamped impact from $H/f_0 \approx 3$ on, it follows the steep curve.

In figure 8 the maximum force with weight-balanced and free-drop impact is compared. In contrast to the conditions for straight spring characteristic curves, the quotients $Q(S_g) = S_{g(\lambda=1)}/S_{g(\lambda=0)}$ with about 0.4 are now only half as great as for the linear curve (ref. 5, fig. 7). This phenomenon is comprehensible without further explanation by a glance at figure 6.

The efficiency η follows from the equation

$$\eta = \frac{H/f_0 + (1 - \lambda)\psi_g}{S_g \psi_g} \tag{27}$$

the interpretation of which is given in figures 9 and 10. The damped diagrams in the practical range of damping are much fuller than the undamped ones. Thus, for $H/f_0 = 2$ and $\delta = 1.5$ the ratio $Q(\eta) = \eta_{(\lambda=1)}/\eta_{(\lambda=0)} = 2.23$. This also is explained by figure 6: for $H/f_0 = 1.5$ the efficiency with 0.95 is nearly equal to unity, whereas the diagram is almost a rectangle. At increasing values of ψ_g, η decreases rapidly; but to the free-drop impact there always corresponds a greater spring travel or stroke ψ_g than to weight-balanced impact (figs. 4 and 5).

The energy absorbed by the strut at the first landing impact is

$$A = H/f_0 + (1 - \lambda)\psi_g \tag{28}$$

whence by equation (19)

$$\frac{A_D}{A} = \frac{\frac{2}{3}\delta\sqrt{H/f_0}\psi_g}{H/f_0 + (1 - \lambda)\psi_g} \tag{29}$$

As indicated by the representation of equation (29) in figure 11, at $\delta = 1.5$ air and damper oil participate about equally in the energy absorption, and which is fairly independent of the height of drop H in the practical range.

Figure 11 and equation (29) show the way by which the damping factor δ can be determined by a test.

With full lift relaxation

$$\frac{\delta\psi_g}{\sqrt{H/f_0}} = 1.5\,\frac{A_D}{A} \tag{30}$$

Simply measure the maximum compression ψ_g for a given height of drop H, and calculate A_F by equation (4) or table 1. Then A can be computed by equation (28) and with $A_D = A - A_F$ the damping factor δ obtained by equation (30). This calculation is further facilitated by figure 12.

With it, the present report is concluded. Whether I am successful in extending the described approximate method to the calculation of oleo-pneumatic legs with tires, I don't know. However, the present three-part total report should, I hope, give not only hints to landing-gear diagrams for construction and test, but also serve to stimulate further research.

Translated by J. Vanier
National Advisory Committee
for Aeronautics

REFERENCES

1. Schlaefke, K.: Zur Kenntnis der Kraftwegdiagramme von Flugzeugfederbeinen. 2. Teilbericht: Näherungsverfahren zum Berechnen der Kraftwegdiagramme mit nichtlinearer Federkennlinie und linearer oder quadratischer Dämpfung. Tech. Berichte, Bd. 11, Heft. 4, April 25, 1944, pp. 105-109. (Presented in this translation as Second Partial Report.)

2. Michael, F.: Theoretische und experimentelle Grundlagen für die Untersuchung und Entwicklung von Flugzeugfederungen. Luftfahrtforsch., Bd. 14, Nr. 8, 1937, pp. 387-416. Abdruck des gleichnamigen Forschungsberichtes FB 87, 1934. Grenzen von fg; p. 395.

3. Irmer, H.: Luftfederung bei Flugzeugen und Kraftfahrzeugen. Z. VDI, Bd. 81, 1937, p. 1182.

4. Hadekel, R.: Shock Absorber Calculations. Aircr. Engr., Bd. 19, Nr. 7 (Flight Bd. 38, Nr. 1648 v. July 25, 1940), p. 71; ZWB-Übersetzung Nr. 2401.

5. Schlaefke, K.: Zum Vergleich von gepufferten und ungepufferten Federstössen an Flugzeugfahrwerken. Techn. Ber., Bd. 10, Nr. 5, 1943, pp. 129-133.

6. Schlaefke, K.: Erfahrungen bei Fallhammer- und Rolltrommelversuchen. Vortrag vor der Lilienthal-Ges., Berlin, 1943.

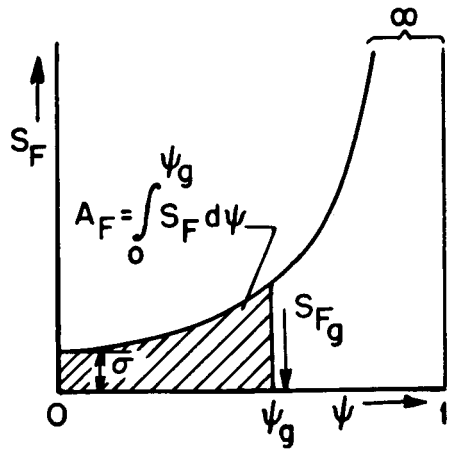

Figure 1.- The compression curves of compressed-air legs.

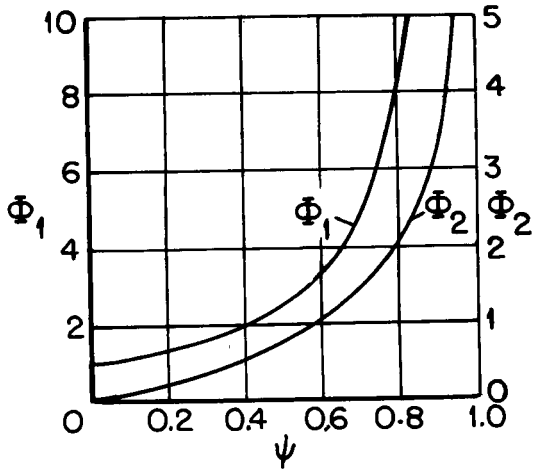

Figure 2.- Functions for calculating the compression curve.

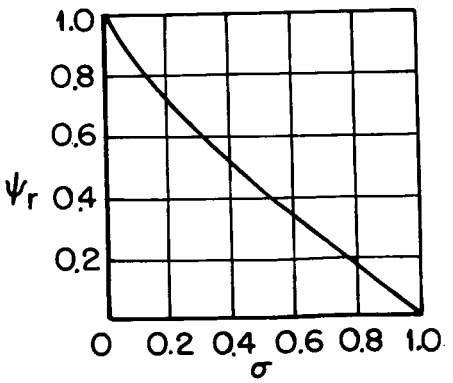

Figure 3.- Initial tension and spring travel under static load.

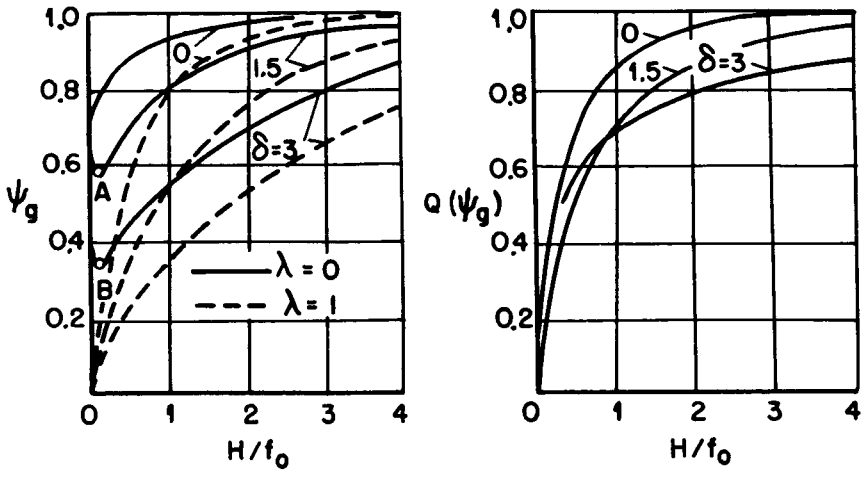

Figures 4 and 5.- Maximum compression of oleo-pneumatic legs at landing impact.

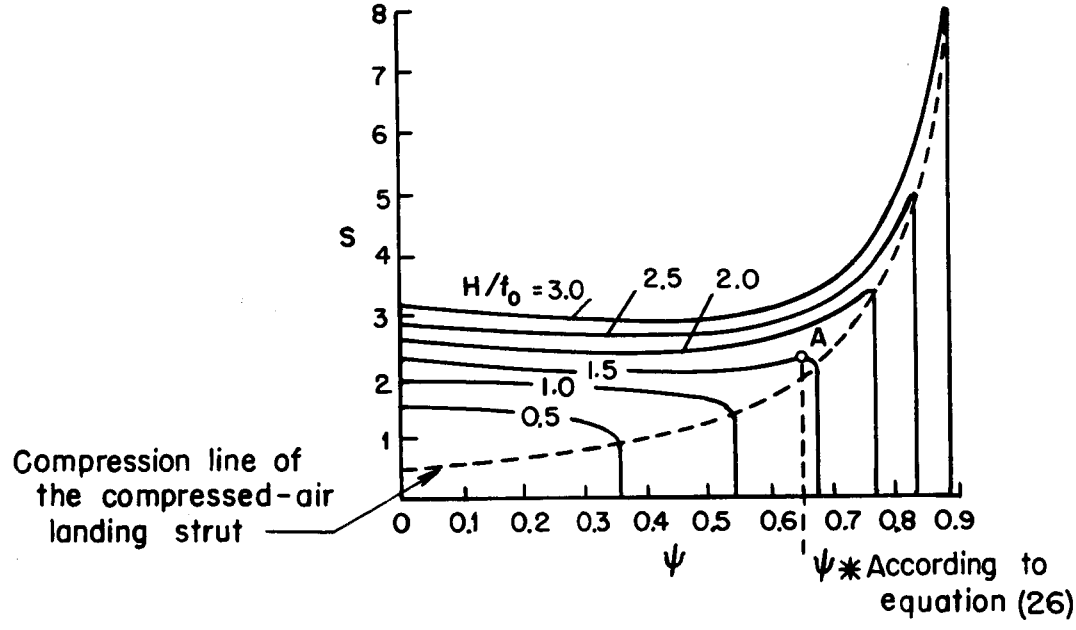

Figure 6.- Examples of force-stroke diagrams for $\delta = 1.5$ and $\lambda = 1$ (complete lift relaxation) at several heights of drop H.

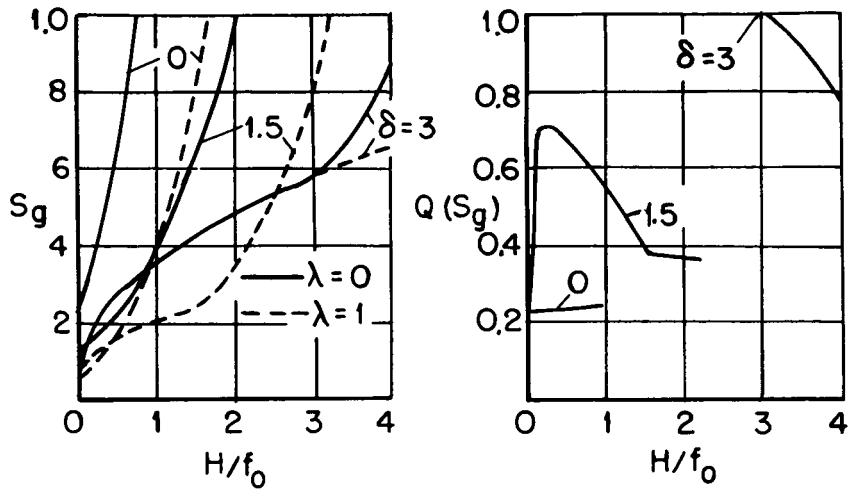

Figures 7 and 8.- Maximum force of oleo-pneumatic legs at landing impact.

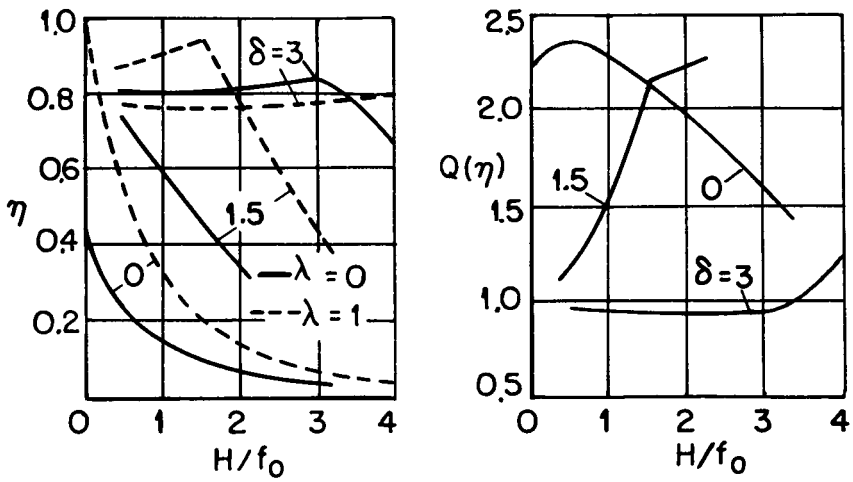

Figures 9 and 10.- Efficiency of force-stroke diagrams of oleo-pneumatic legs at landing impact.

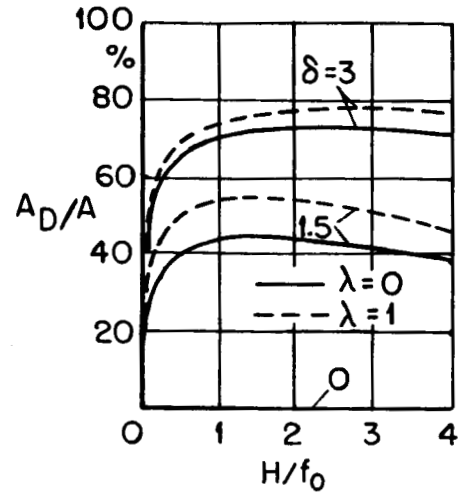

Figure 11.- Proportion of oil damping energy to total energy.

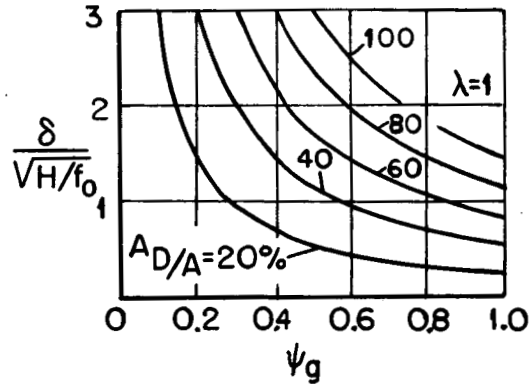

Figure 12.- Diagram for determining the damping δ from the test values H, ψ_g and A_D/A.